CrossMark

Efficient adsorption toward precious metal from aqueous solution by zeolitic imidazolate framework-8

Chenghong Hu[1] · Weifeng Xu[1] · Xiaohui Mo[1] · Hua Li[1] · Siman Zhou[1] · Panliang Zhang[1] · Kewen Tang[1]

Abstract

The recycling of precious metal ions is highly desirable to the environment and economy. In this work, zeolitic imidazolate framework-8 (ZIF-8), a porous and relatively stable adsorption material, was explored for the adsorption of Au from water. Important conditions affecting the adsorption performance were investigated, including pH, adsorption time, initial concentration, and temperature. In consequence, the ZIF-8 adsorbent exhibits excellent adsorption performance toward Au(III) with high adsorption capacity of 1192 mg g^{-1} at pH 2.5 and 298 K. In addition, the study of recycling use indicated that the stable adsorption performance being maintained after recycle twice. The adsorption process of Au(III) onto ZIF-8 undergoes a spontaneous endothermic process and fits well with the Freundlich isotherm model. Kinetics studies indicated that the kinetics follows pseudo-second-order model and the intraparticle diffusion is the adsorption rate-determining step. Mechanism studies suggested that the electrostatic interaction and partial reduction of Au(III) play vital roles in the adsorption process. This work introduces a promising adsorbent for Au separation due to its considerable adsorption capacity, outstanding stability, and facile regeneration.

Keywords Precious metal recovery · ZIF-8 · Adsorption · Mechanism · Recycling

1 Introduction

Most of precious metals with beautiful colors such as Au, Ag, and Pt have strong chemical stability which hardly react with other chemicals in general conditions. Specifically, Au has excellent physicochemical properties, such as the resistance to high temperature oxidation and corrosion, outstanding electrical conductivity, highly catalytic activity, strong coordination ability, and so on. Hence, Au is widely used as industrial vitamin. The shortage of supply and high industrial demand highlights the recycling of Au from secondary resources (Wang et al. 2017).

Presently, many methods have been applied in the separation of precious metal ions including adsorption, chemical precipitation, ion exchange, membrane filtration, and biological method (Kavakli et al. 2006; Zhang et al. 2015; Shams and Goodarzi 2006; Gwak et al. 2018; Dobson and Burgess 2007). Among them, adsorption is the most widely used method due to the comparatively cost-effective, simplicity of design, facile operation, and low amount of harmful secondary products (Lin et al. 2017; Zhang and Xu 2016). Amidst the widely practical adsorbents for retrieving precious metals, activated carbon, bioadsorbent are the most widely used. Gold recovery form leaching solutions by adsorption onto activated carbon has been the dominant process due to the porosity and large specific surface area of the activated carbon; while the hard regeneration and low selectivity limits the application (Fleming et al. 2011; Mpinga et al. 2014). Biosorbents, especially microorganisms, has shown good sorption capacities towards precious metals (Maruyama et al. 2014; Chen et al. 2011). However, the microorganism based biosorbents have many drawbacks, such as poor acid tolerance, poor mechanical strength and little rigidity, difficulty in solid–liquid separation (Won et al. 2014). The immobilized biosorbents have been attempted to solve these problems, but simultaneously having the strong acidity stability, high sorption capacity, good selectivity toward gold and excellent reutilization is still challenging

---

Chenghong Hu and Weifeng Xu equally contributed to the work.

✉ Kewen Tang
tangkewen@sina.com

1. Department of Chemistry and Chemical Engineering, Hunan Institute of Science and Technology, Yueyang 414006, Hunan, China

(Ramesh et al. 2008; Ogata and Nakano 2005). Additionally, the immobilization process may increase additional process cost and mass transfer limitation between the solute and the immobilized sorbent. Therefore, exploring efficient adsorbents is in great demand.

Metal–organic frameworks (MOFs) is a versatile porous material formed through coordination between metal ions and multi-type organic ligands. MOFs with the characteristics of high degree of pore structure, high surface area and adjustable pore size, thus leading to intense application in gas storage (Sumida et al. 2011), catalysis (Shen et al. 2018), drug delivery (Horcajada et al. 2012), optics (Cui et al. 2012), and sensing (Ghosh 2017), especially in separations (Li et al. 2011). However, the separation of precious metal from water by MOFs received little prior attention. Wu and coworkers adopted thiourea modified zirconium-based MOFs (UiO-66-TU) to adsorb Au(III) from the waste electronic and electrical equipment (WEEE) (Wu et al. 2017), and the maximum Au adsorption capacity was 326 mg g^{-1}. Zha and coworkers employed ASUiO-66 constructed from Zr(IV) ions and the linker 2,6-bis(allylsulfanyl)terephthalic acid to selectively recover Pd from water, and the saturation capacity was 45.4 mg g^{-1} (Zha et al. 2015). The above MOFs reveal good identification performance toward precious metal, while the adsorption capacity is unsatisfactory. Zeolitic imidazolate frameworks (ZIFs) are an emerging class of porous materials and widely used in gas adsorption, removal of organic compounds and heavy metals from solution, due to its structural integrity (Jiang et al. 2013), excellent stability (Niknam et al. 2017) and large pore size (Zhang et al. 2013). ZIFs were reported to act as a molecular sieve with the properties termed the rotary door effect (Gücüyener et al. 2010). Specifically, there are abundant alkaline and acid functional groups residing on the external surface, such as alkaline hydroxyl groups offered by OH^{-1} and N^{-1}, Lewis acid sites from low coordinated Zn, and Brønsted acid sites related to –NH (Chizallet et al. 2010). The enough large surface areas and abundant functional groups on the surface may provide an alternative approach to selectively adsorb the precious metal.

Herein, we report on ZIF-8 as highly effective adsorbent for adsorption Au from aqueous solution. The structure of ZIF-8 was characterized by multiple measurements techniques including powder X-ray diffraction spectrometry (PXRD), N$_2$ adsorption–desorption methods, and thermogravimetric analysis (TGA). To gain the optimal absorption activity, we investigated the influence factors including pH, contact time, temperature, and initial concentration in detail. The recycling use of ZIF-8 was also studied and the stability of its structure was verified by PXRD and Fourier transform infrared spectrometer (FT-IR). Further, the materials before and after adsorption were measured by transmission electron microscope (TEM), energy-dispersive X-ray spectroscopy (EDS), and X-ray photoelectron spectroscopy (XPS) to confirmation of the absorption of Au on ZIF-8.

2 Materials and methods

2.1 Materials and preparation

N,N-dimethylformamide (DMF) was purchased from Shanghai Titan Scientific Co., Ltd (Shanghai, China, 99.5%). 2-methylimidazole was obtained from Adamas-beta Co., Ltd (Shanghai, China, 98%). Zinc nitrate hexahydrate (Zn(NO$_3$)$_2$·6H$_2$O) was acquired from Sinopharm Chemical Reagent Co., Ltd (Beijing, China, AR). AuCl$_3$ was provided by Energy Chemical Co., Ltd (Shanghai, China, 98%). Acetonitrile was purchased from Sigma-Aldrich Co., Ltd (Beijing, China, 99.9%). All chemicals from commercial sources were of reagent grade and used without further purification, and all solutions were prepared with deionized water.

ZIF-8 was obtained by the modification of a literature procedure (Jiang et al. 2016). Zn(NO$_3$)$_2$·6H$_2$O (2.5 mmol) and 2-methylimidazole (7.5 mmol) were dissolved into DMF (600 mL) in the boiling flask-3-neck sealed with a glass stopper. The mixture was stirred until the solid was completely dissolved, and then placed in a silicon oil bath at 413 K for 24 h without stirring. After cooling the solution to room temperature, the mixture was filtered to get a solid product, and then the solid was washed with methanol for three times. The final product was obtained as a brownish black power by dried the solid in a vacuum oven at 353 K for overnight.

2.2 Adsorption process

A series of batch experiments were carried out to investigate the adsorption performance of ZIF-8 toward Au(III). Aqueous solutions were prepared by dissolving amount of AuCl$_3$ solid into deionized water, then the solutions were adjusted to the targeted pH recorded at a meter (China Leici Co. Ltd., PHSJ-3F) by 0.1 mol L^{-1} NaOH or HCl. For pH effect studies, the used pH varied from 2.5 to 12. For adsorption measurements, 10 mg ZIF-8 was added into 20 mL solution containing 250 mg L^{-1} Au(III) in 50 mL centrifuge tube at 298 K. For adsorption kinetic analysis, additional solutions were prepared by dissolving 50 mg ZIF-8 into 100 mL 300 mg L^{-1} Au(III) solution at the temperature of 298 K. Adsorption isotherm study was performed by adding 10 mg ZIF-8 into the varied concentration solution of Au(III) from 10 mg L^{-1} to 900 mg L^{-1} at pH 2.5 and 298 K. For thermodynamic studies, 10 mg ZIF-8 materials were added into 20 mL 400 mg L^{-1} Au(III) solution with a range of temperature from 278 K to 318 K. All the centrifuge tubes or conical flask are placed in the Thermostatic oscillator in freezing waters to vibrate for adsorption.

2.3 Recycling studies

To study the recovery performance of ZIF-8 materials, many methods have been used to desorb metal ions from the as-used ZIF-8, such as changing the pH of aqueous solution (Li et al. 2014), using the organic solvent (Jiang et al. 2016), and so on. In this work, acetonitrile was chosen as the desorption solvent. The experimental procedure was as follows: 150 mg ZIF-8 was added into 100 mL solution containing 300 mg L^{-1} Au(III) with oscillation 48 h at 298 K, and then the adsorbed ZIF-8 was percolate and rinsed repeatedly three times with deionized water. With dried in a vacuum oven at 373 K for 4 h, the recovered ZIF-8 was dissolved in 100 mL acetonitrile vibrating 24 h. Repeat the adsorption–desorption experiments and study the adsorption capacity to verify the recovery performance of ZIF-8.

2.4 Analytical methods

The concentration of Au(III) ion in solution was measured through atomic adsorption spectroscopy (AAS, Japan Shimadzu Co. Ltd., AA-6880). The adsorption capacity (q_e, mg g^{-1}) of Au(III) on ZIF-8 at equilibrium and at time t (q_t, mg g^{-1}), as well as the removal ratio (R %) were calculated by the following Eq. (1–3).

$$q_e = \frac{(C_0 - C_e) \times V}{m} \tag{1}$$

$$q_t = \frac{(C_0 - C_t) \times V}{m} \tag{2}$$

$$R\% = \frac{(C_0 - C_t)}{C_0} \times 100 \tag{3}$$

where C_0 (mg L^{-1}) and C_t (mg L^{-1}) represent the initial concentration and concentration at time t (min) of Au, respectively. C_e (mg L^{-1}) represents the equilibrium concentration of Au in the solution. V is the adsorption volume (mL), and m is the quality of adsorbent (mg).

2.5 Instrumentation

The crystallinity and phase information of the self-assembly ZIF-8 was measured by powder X-ray diffraction spectrometry (PXRD) equipped with a D/max-2500 diffractometer (Rigaku, Japan) using Cu K$_\alpha$ radiation (λ = 1.5418 Å) over 2θ from 5° to 50°. The Brunauer–Emmett–Teller (BET) surface, pore volume and pore size distribution of adsorbents were calculated by using the N$_2$ adsorption–desorption methods (ASAP2020, US). Thermogravimetric analysis (TGA) was performed on a PTC-10A thermal gravimetric

analyzer (Rigaku, Japan) ranging from room temperature to 1173 K at a ramp rate of 5 °C min^{-1}. The infrared spectrum was recorded on a Fourier transform infrared spectrometer (FT-IR, Avatar 370, Thermo-Nicolet, USA) in the range of 400–4000 cm^{-1}. The X-ray photoelectron spectroscopy (XPS) measurements were recorded on a Kratos Axis Ultra DLD spectrometer fitted with a monochromated Al Kα X-ray source (hν = 1486.6 eV), hybrid (magnetic/electrostatic) optics, and a multichannel plate and delay line detector (Kratos, Manchester, UK). The elemental compositions of the samples were characterized by energy-dispersive X-ray spectroscopy (EDS, Oxford instruments X-Max, UK). The transmission electron microscope (TEM) image was recorded on a Tecnai G^{2}20 transmission electron microscope (FEI, Japan) operating at a 100 kV accelerating voltage.

3 Results and discussion

3.1 Characterization of the Absorbents

The synthesized ZIF-8 was first detected by PXRD. As shown in Fig. 1a, the three distinct characteristic peaks located at 7.36°, 12.7°, and 18°, which were in good agreement with the theoretical computational values and the published experimental data (Jiang et al. 2016). The result confirmed the successful preparation of the ZIF-8 material. The TGA curve of ZIF-8 was shown in Fig. 1b. The mass loss of 12.6% below 473 K was attributed to the removal of residual DMF molecule, and some 2-methylimidazole attached to surface of materials. The self-synthesized materials start to collapse and break down at about 523 K, which is different from the reported result that the stability of ZIF-8 can reach 723 K (Li et al. 2014). This may be caused by the adjustment of solvent ratio in the synthesis process. The N$_2$ adsorption–desorption isotherm of as-synthesized ZIF-8 shows a characteristic Type I adsorption behavior (Fig. 1c), which is consistent with the previous report (He et al. 2014). The BET specific surface area is determined as 1291.8 m^2 g^{-1}. The pore size distribution based on the Barrett–Joyner–Halenda (BJH) model of ZIF-8 is shown in Fig. 1d, which indicates a pore size distribution ranged from 10 to 70 nm with a pore diameter and volume of 34.8 nm and 0.5245 cm^3 g^{-1}, respectively. The TEM image was displayed in Fig. 1e. ZIF-8 appears as a hexagonal shape, which is consistent with the literature (Li et al. 2014). The FT-IR results of ZIF-8 in the range of 4000–400 cm^{-1} are displayed in Fig. 1f. The strong band in the spectral region of 2580–3630 cm^{-1} is ascribed to C–H, N–H and O–H stretching vibrations of methyl, hydroxyl and amine groups on ZIF-8 materials (And and Nuzzo 1992). The peak at 1350–1500 cm^{-1} can be assigned to the stretching of the ring of the 2-methylimidazole (Hu et al. 2011). In addition,
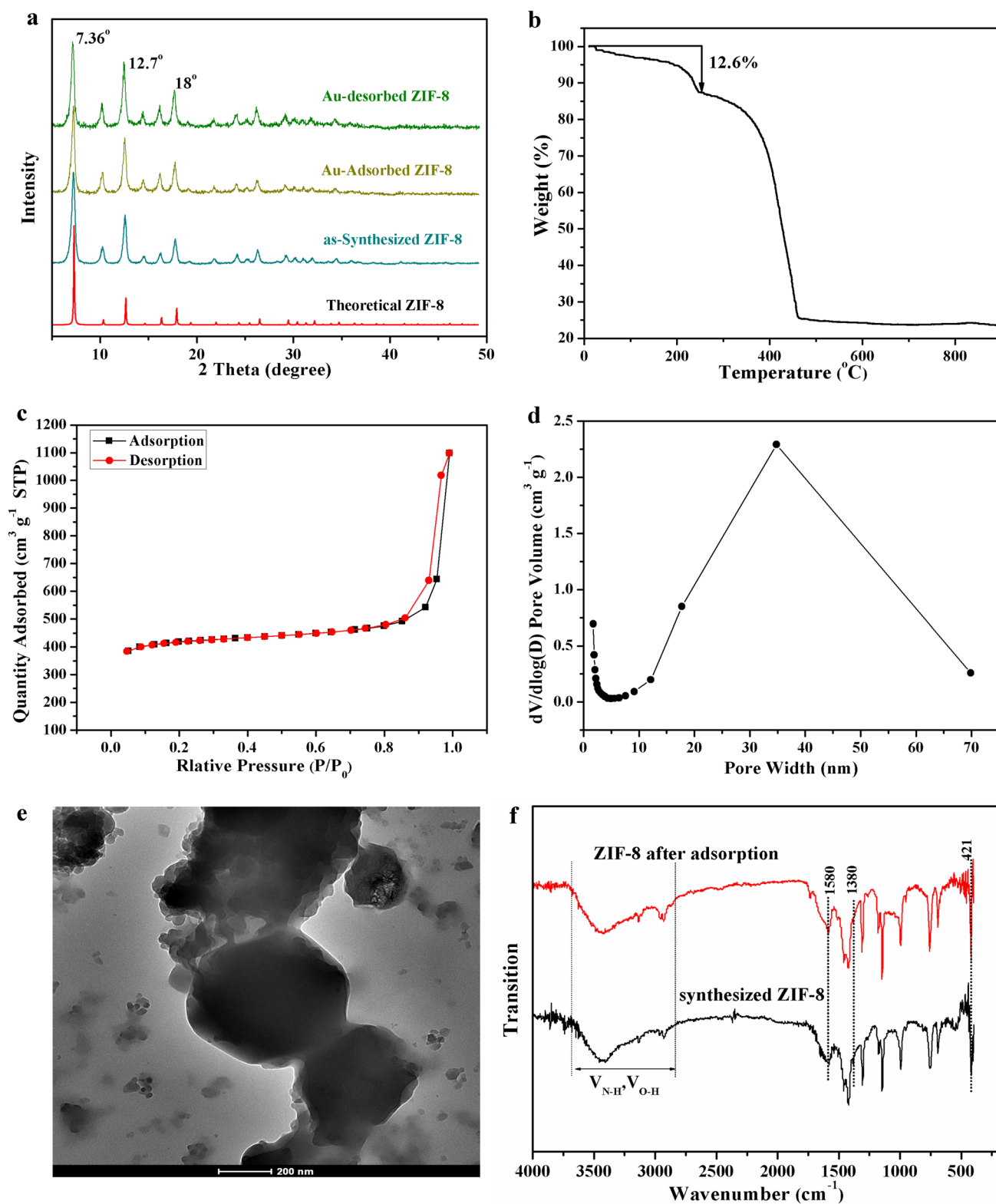
Fig. 1 **a** Simulated and as-synthesized PXRD patterns of ZIF-8. **b** TGA trace of compound ZIF-8. **c** Nitrogen adsorption–desorption isotherms. **d** Pore diameter of ZIF-8 calculated by BJH method. **e** TEM image of ZIF-8. **f** FTIR spectra of ZIF-8 before and after Au(III) adsorption

some characteristic peaks, for example, ~ 421 cm^{-1} (Zn–N) and 1580 cm^{-1} (stretching vibration of C=N), 1380 cm^{-1} (–CH$_3$ bending) can also be observed (He et al. 2014; Liu et al. 2015).

The structure of ZIF-8 after adsorption was characterized by FT-IR and PXRD. By observing the infrared chromatogram after adsorption, there is no new distinct peak appears (Fig. 1f). It can also be clearly observed that identical peaks of the Au-adsorbed ZIF-8 match well with the as-synthesized ZIF-8 without other crystalline phase appearing (Fig. 1a). It prove that stability of ZIF-8 was kept during the adsorption process.

3.2 Effect of pH on the adsorption of Au(III)

The pH of the solution is a crucial factor for metal ion adsorption, since it can affect the stability and surface charged mode of the material in the solution. The dependence of adsorption capacity (q_e) on pH was investigated in the pH range of 2.5–12. As shown in Fig. 2, the adsorption capacity decreases rapidly with the increase of pH value, and it decreases to zero when pH is at 12.

Given that AuCl$_3$ is prone to hydrolyze in an aqueous solution as shown in the Eq. (4) with a constant k of $10^{-0.7}$ (Mironov and Makotchenko 2009; Robb 1967), where k is expressed by Eq. (5).

$$AuCl_3 + H_2O \overset{k}{\rightleftharpoons} AuCl_3OH^- + H^+ \quad (4)$$
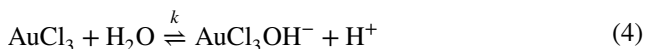
$$k = \frac{[AuCl3OH^-][H^+]}{[AuCl3]} \quad (5)$$

In this experiment, the initial pH was 2.5, and then we can calculate that ratio of [AuCl$_3$(OH)$^-$] to [AuCl$_3$] is 63, which means that the predominant complex of Au(III) is AuCl$_3$(OH)$^-$. As the pH goes up, the ratio is going to

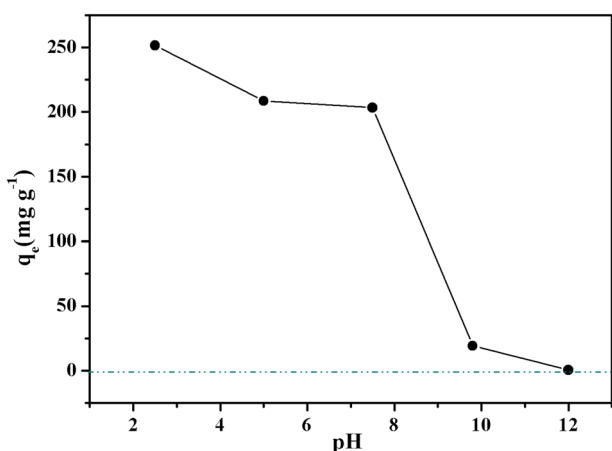**Fig. 2** Adsorption capacity dependence on pH. (Conditions: $m = 10$ mg, $C = 250$ mg L^{-1}, V = 20 mL, $t = 42$ h, T = 298 K)

increase. When pH 12, the ratio value equals to 1.9×10^{11}. Hence, we can conclude that in the pH range studied, the anion AuCl$_3$(OH)$^-$ is the main existence form.

In a previous study, the zeta potential decreased with the pH value increased and the isoelectric point of ZIF-8 is at around pH 10 (pH$_{pzc}$), which indicates that ZIF-8 is positively charged in the pH range of 2.5–10 (Jian et al. 2015). This phenomenon is consistent with that in the adsorption experiment, in which the adsorption ability of ZIF-8 toward Au(III) was highly pH dependent and only small amount of Au(III) was adsorbed with pH value being above 10. The positive site groups can be formed by the N atoms of ZIF-8 through protonated reaction (e.g. C=NH$^+$, C=NH$_2^+$) below the pH$_{pzc}$, which have propensity to combine with the negative AuCl$_3$(OH)$^-$ species via electrostatic interaction. Therefore, it can be indicated that the electrostatic interaction may have a very prominent influence on the adsorption of Au onto ZIF-8.

3.3 Adsorption kinetics studies

Figure 3 displays the dependence of adsorption capacity on time. It can be obvious found that the adsorption capacity increases rapidly at the beginning, and then increases slowly. The adsorption equilibrium is achieved within 42 h with the maximal capacity of 434 mg g^{-1}. The adsorption kinetics of Au(III) ions onto ZIF-8 was described by pseudo-first-order (Eq. 6) and pseudo-second-order (Eq. 7):

$$\log(q_e - q_t) = \log q_e - \frac{k_1 t}{2.303} \quad (6)$$

$$\frac{t}{qt} = \frac{1}{k_2 q_e^2} + \frac{t}{qe} \quad (7)$$

where k_1 (min^{-1}) and k_2 (g mg^{-1} min^{-1}) is the pseudo-first-order and pseudo-second-order rate constant, respectively. The related parameters are listed in Table 1. As shown in Fig. 4, the kinetics greatly fits the pseudo-second-order model ($R^2 = 0.9981$), which indicates that chemisorption is significant in the rate-limiting step (Ho and McKay 1999), involving exchanges or sharing of electrons between Au(III) and ZIF-8.

Furthermore, the moving boundary model was used to differentiate the relative roles of adsorption steps involved to play. If the adsorption process was controlled by liquid film diffusion, intraparticle diffusion or chemical interaction, the rate constant can be expressed by Eqs. (8–10) (Liu et al. 2011).

$$k_1 = -\ln(1 - F) \quad (8)$$

$$k_2 = 1 - 3(1 - F)^{2/3} + 2(1 - F) \quad (9)$$

$$k_3 = 1 - (1 - F)^{1/3} \quad (10)$$

where F is the adsorption fraction (q_t/q_e), and k is the adsorption rate constant. By plotting a linear relationship

Fig. 3 The adsorption capacity varies with time. (Conditions: $m = 10$ mg; $C = 300$ mg L^{-1}, V = 100 mL, T = 298 K, pH = 2.5)
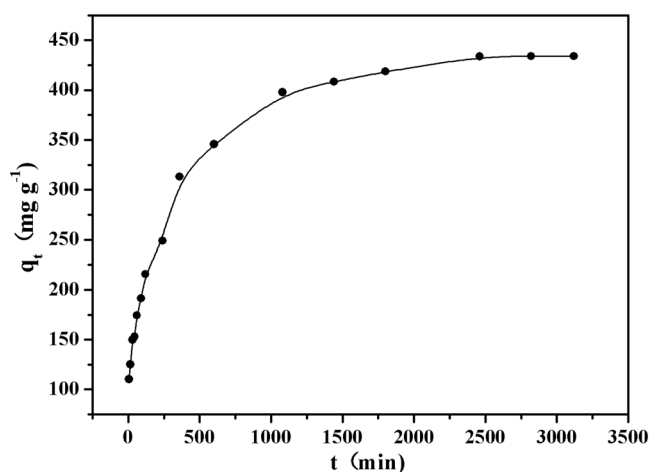

Table 1 Adsorption kinetic parameters for the Au(III) adsorption onto the ZIF-8

C_0 (mg L^{-1})	q_e,exp (mg g^{-1})	Pseudo-first-order model			Pseudo-second-order model		
		q_e, cal (mg g^{-1})	k_1 (min^{-1})	R^2	q_e, cal (mg g^{-1})	k_2 (g mg^{-1} min^{-1})	R^2
300	434	380.1	0.00265	0.9551	454.5	2.2×10^{-5}	0.9980

of k versus contact time t (min), the regression coefficients (R^2) for three adsorption steps were obtained, of which the one with the highest R^2 value was intended to be the rate-determining step. The fitted linear regression results show that the R^2 for Eqs. (8–10) are 0.9214, 0.9740 and 0.9640. The highest R^2 value for Eq. (9) indicates that the Au(III) adsorption rate mainly be controlled by intraparticle diffusion. In addition, concomitant high R^2 value for Eq. (10) suggests that chemical interaction also play an important role in the adsorption rate-determining step.

3.4 Adsorption isotherms investigation

The relationship between the adsorption of Au ion by ZIF-8 and the equilibrium Au(III) concentration in solution is depicted in Fig. 5. It is clear that the adsorption performance of ZIF-8 depends on the Au(III) concentration. The maximal adsorption capacity can reach 1192 mg g^{-1} in this work. A comparison of the adsorption capacities of Au(III) by various materials is shown in Table 2. The result illustrates that ZIF-8 exhibit better adsorption capability than many reported adsorbents. In a recent study, ZIF-8 was modified by sulfur derivatives reveals outstanding coordination ability with precious metals (Wang et al. 2018), which indicates the excellent potential of ZIF-8 for recovery precious metal ions.

The Langmuir and Freundlich isotherm model are used to depict the adsorption process (Eqs. 11, 12).

$$\frac{C_e}{q_e} = \frac{C_e}{q_m} + \frac{1}{K_L q_m} \tag{11}$$

$$\ln q_e = \ln K_F + \frac{1}{n} \ln C_e \tag{12}$$

where q_m is the maximum adsorbed capacity toward Au by ZIF-8 and K_L is a Langmuir constant related to the affinity of binding sites (L mg^{-1}). K_F and n are Freundlich constants related to the adsorption capacity and adsorption intensity, respectively. The adsorption isotherm and basic parameters of the isotherm equations are shown in Fig. 6 and Table 3. The results in Table 3 manifest that the Freundlich isotherm fits the Au(III) adsorption isotherm well with $R^2 = 0.9263$, which is better than that of the Langmuir isotherm with $R^2 = 0.664$. Therefore, it can be suggested that the ZIF-8 adsorption of Au(III) was a heterogeneous sorption (Jian et al. 2015).

3.5 Adsorption thermodynamics

The temperature is an important factor for adsorption process. As shown in Fig. 7a, adsorption capacity of ZIF-8 toward Au(III) keeps growing as temperature increases from 278 to 318 K. We also examined the thermodynamics parameters of gibbs free energy change (ΔG, kJ mol^{-1}), enthalpy change (ΔH, kJ mol^{-1}), and entropy change (ΔS, kJ mol^{-1}) during adsorption process, which were calculated by the following Eqs. (13–15) (Biggar and Cheung 1973; Huo and Yan 2012).

$$K_0 = \frac{q_e}{C_e} \tag{13}$$

$$\Delta G = -RT \cdot \ln K_0 \tag{14}$$

a

$$\log(q_e-q_t)=2.5809-0.00115t$$
$$R^2=0.9551$$

b

$$t/q_t=0.2394+0.0022t$$
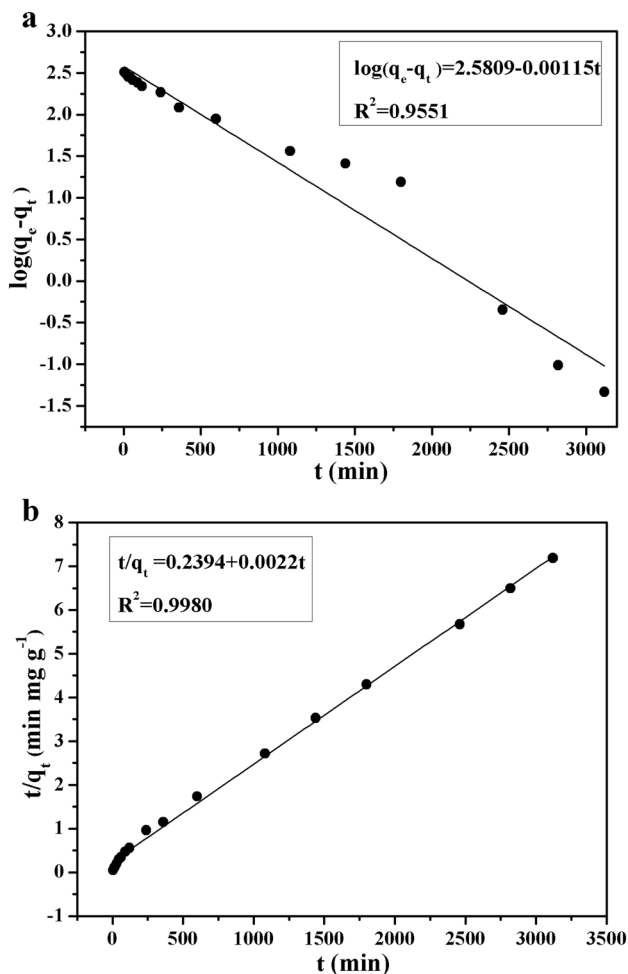$$R^2=0.9980$$

Fig. 4 **a** Pseudo-first-order and **b** pseudo-second-order kinetics plots of Au(III) adsorption onto the ZIF-8
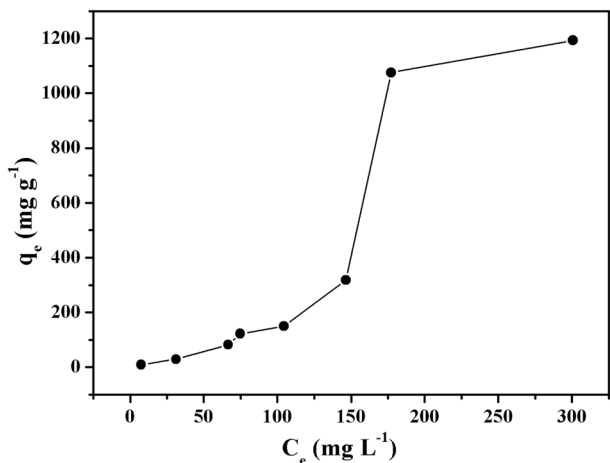

Fig. 5 The adsorption capacity connected with equilibrium concentration. (Conditions: $m=10$ mg, V $=20$ mL, $t=42$ h, T $=298$ K, pH $= 2.5$)

Table 2 Comparison of the adsorption capacities of Au onto various adsorbent

Adsorbent	q_{max} (mg g^{-1})	Refs.
ZIF-8	1192	This work
Chitosan	30.95	Ngah and Liang (1999)
Taurine modified cellulose	34.5	Dwivedi et al. (2014)
Porous carbon	90.6	Chand et al. (2009)
Glycine modified chitosan resin	170	Ramesh et al. (2008)
UiO-66-TU	326	Wu et al. (2017)
UiO-66-NH$_2$	495	Lin et al. (2017)

a

$$C_e/q_e=-0.0027C_e+0.9202$$
$$R^2=0.664$$

b

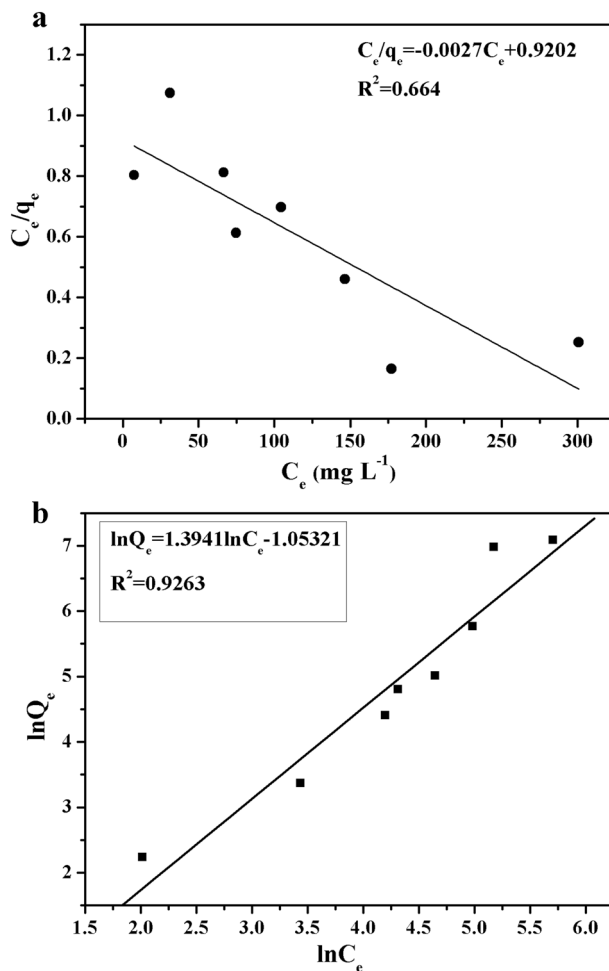$$\ln Q_e=1.3941\ln C_e-1.05321$$
$$R^2=0.9263$$

Fig. 6 Langmuir (**a**) and Freundlich (**b**) isotherm model fitting curves of Au(III) adsorption onto the ZIF-8

$$\ln K0 = \frac{\Delta S}{R} - \frac{\Delta H}{RT} \tag{15}$$

where K_0 is the thermodynamic equilibrium constant. R (8.314 J mol^{-1} K^{-1}) is the ideal gas constant, and T (K)

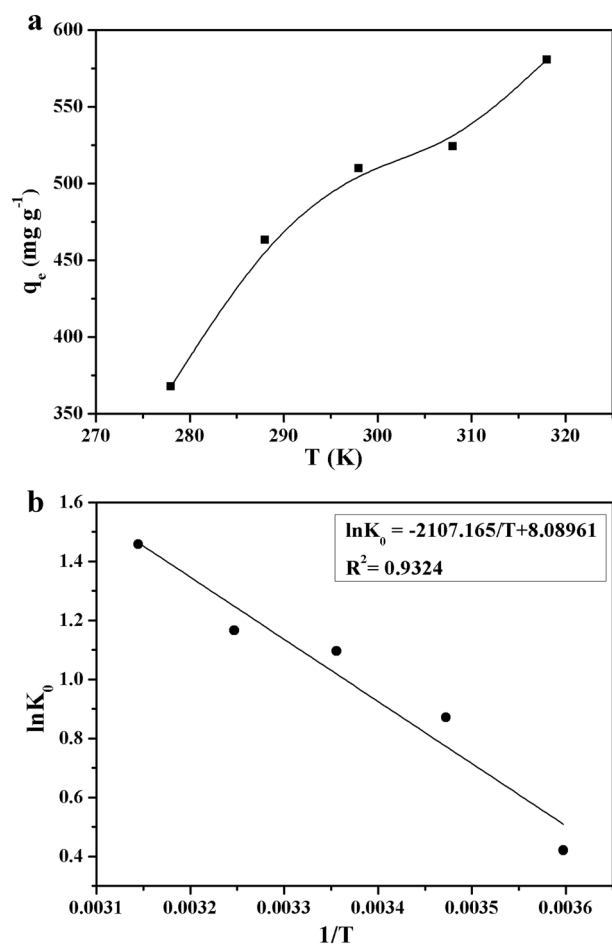**Table 3** Adsorption isotherm parameters for the Au(III) adsorption onto the ZIF-8

Langmuir			Freundlich		
K_L (L mg^{-1})	q_m (mg g^{-1})	R^2	K_F	n	R^2
− 0.003	− 370.37	0.664	0.349	0.717	0.9263

Table 4 Thermodynamic parameters for the Adsorption of Au(III) onto ZIF-8

T (K)	ΔG (kJ mol^{-1})	ΔH (kJ mol^{-1})	ΔS (kJ mol^{-1} K^{-1})
278	− 0.9733	17.52	0.0673
288	− 2.086		
298	− 2.715		
308	− 2.985		
318	− 3.856		

Table 5 Characterization of the ZIF-8 before and after adsorption

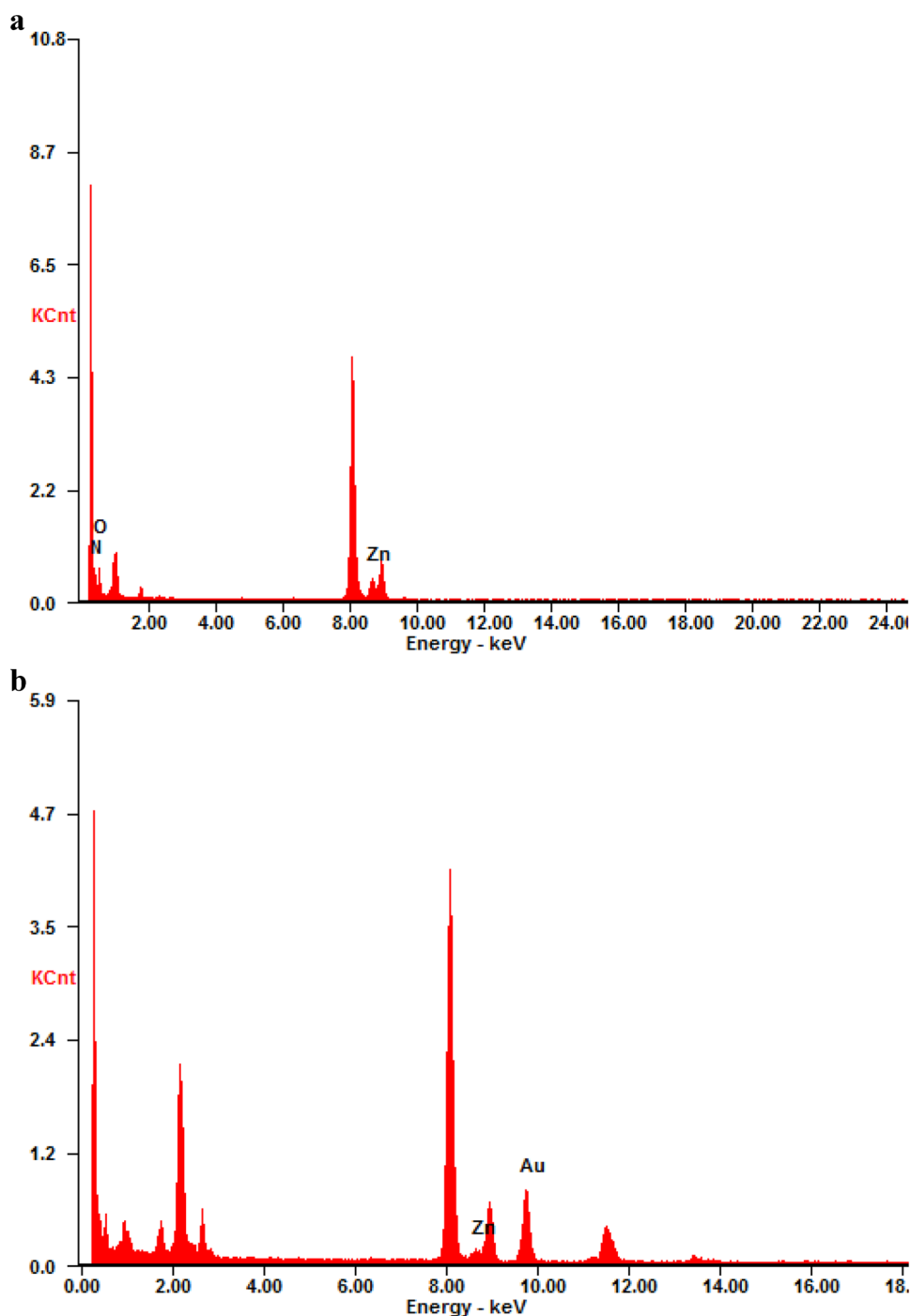|	Before adsorption	After adsorption
BET surface area (m^2 g^{-1})	1291.8	686.04
Micropore Area (m^2 g^{-1})	1015.9	482.06
External surface area (m^2 g^{-1})	275.89	203.98
Micropore volume (cm^3 g^{-1})	0.5245	0.2492

The positive ΔH is unsuitable for spontaneous adsorption process, but the positive ΔS is suited for it. Hence, entropy effect is the predominant driving force for the Au(III) adsorption on ZIF-8 (Lyu et al. 2017).

3.6 Proposed mechanisms

As aforementioned, at a pH higher than pH_{zpc}, there are still small capacities of Au adsorption, which means other ways besides for electrostatic attraction may take effect in the adsorption process of Au onto ZIF-8. To gain insight into the adsorption mechanism, a series of measurements were used to detect the changes in surface properties of adsorbent before and after adsorption. After Au(III) adsorption, N_2 adsorption–desorption measurement showed that the micropore area and volume of the ZIF-8 decreased sharply (Table 5), varying from 1015.9 m^2 g^{-1} to 482.06 m^2 g^{-1}, and from 0.5245 cm^3 g^{-1} to 0.2492 cm^3 g^{-1}, respectively, while the external surface area had a slight change, thus verifying the primary binding sites are at the internal surface of pores. The new emerging peak indexed to Au by EDS measurement after adsorption prove that Au indeed adsorbed on the surface of the ZIF-8 (Fig. 8).

The XPS analysis was further used to characterize the surface chemical composition and states of the ZIF-8 before and after Au(III) adsorption. As shown in Fig. 9a, b, Au 4f core level peak appears in the spectra of ZIF-8 after Au(III) adsorption. As shown in Fig. 9c, d, the high resolution XPS spectra of N 1 s and O 1 s reveals obvious shift after Au adsorption onto ZIF-8, indicating that electron transfer occurred during the adsorption process and partial Au(III) was reduced to low valence state. Therefore, chemical

Fig. 7 Effect of temperature on the adsorption of Au(III) onto the ZIF-8.(conditions: $m = 10$ mg, $t = 42$ h, $C = 400$ mg L^{-1}, V = 20 mL, pH = 2.5)

is adsorption temperature in Kelvin. The ΔH and ΔS were obtained by ln K_0 against $1/T$ in Fig. 7b. The corresponding values are listed in Table 4. The negative ΔG and positive ΔH indicates that the Au(III) adsorption on ZIF-8 is a spontaneous and endothermic process, which is similar with the result reported in other studies (Akpomie et al. 2012; Wang et al. 2017). This phenomenon reveals that chemical adsorption emerges in the adsorption process, which is consistent with the kinetics study. The positive ΔS (0.0673 kJ mol^{-1} K^{-1}) means increasing randomness at the solid-solution interface during adsorption process.

Fig. 8 **a, b** EDS spectra of the ZIF-8 before and after adsorption

adsorption mechanism is also proposed combination of kinetics study and XPS analysis.

On the basis of the aforementioned experimental results and analysis, the proposed adsorption process was put forward: the negatively charged $AuCl_3(OH)^-$ species formed by the hydrolysis and the positive groups ($C=NH_2^+/C=NH^+$) on ZIF-8 generated by protonated reaction interacted with each other through electrostatic interaction, thus leading to the formation of the gold-containing inner complex.

Further, the partial adsorbed Au on the surface of the ZIF-8 is reduced to a low valence state.

3.7 Recycling utilization of the as-synthesized ZIF-8

Regarding of large-scale application in industrial production, reproducible utilization of the adsorbent is in great demand. In a typical experiment, we examined the ability to recycle by desorption the Au from ZIF-8 with the assist
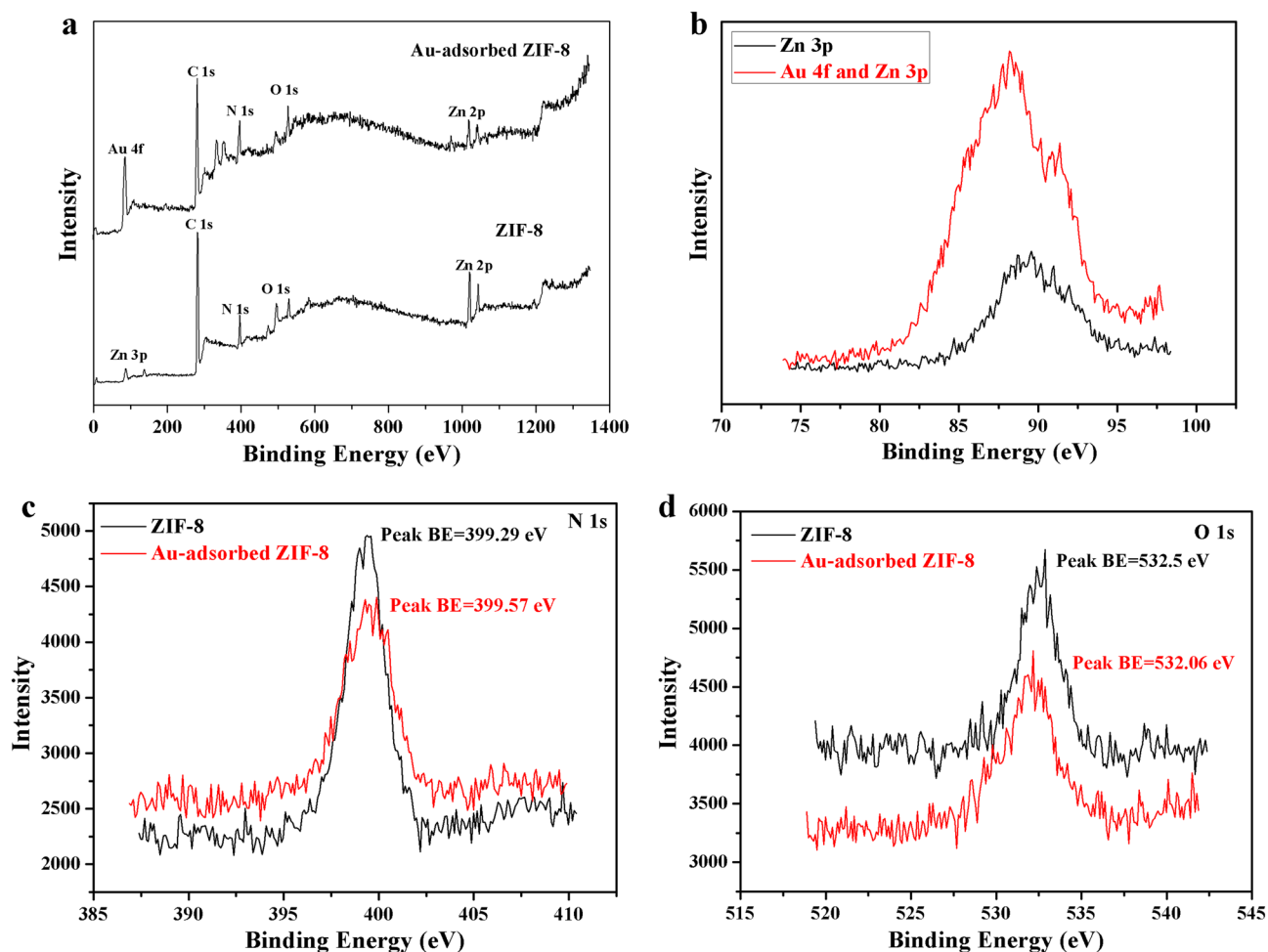
Fig. 9 **a** Survey XPS spectra, **b** Au 4f and Zn 3p, **c** N1s, **d** O 1 s XPS spectra comparison of the ZIF-8 before and after Au(III) adsorption process
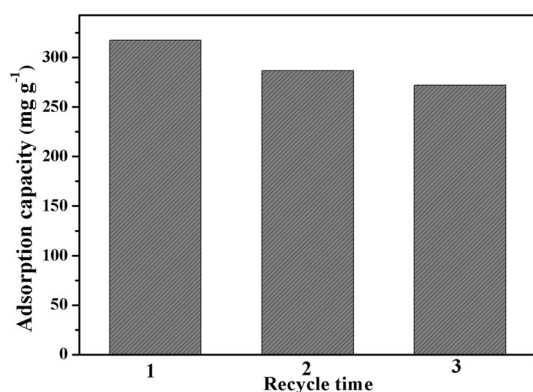

Fig. 10 Recycling utilization of ZIF-8 for Au adsorption. (Conditions: $m = 150$ mg, $V = 100$ mL, $C = 300$ mg L^{-1}, T = 298 K, $t = 42$ h)

of acetonitrile and adsorption of Au in water repeatedly. As shown in Fig. 10, the as-used ZIF-8 exhibits a similar adsorption capacity compared with the fresh one, with 14%

loss of adsorption capacity, manifesting the robustness of ZIF-8 toward Au adsorption. Moreover, the PXRD pattern of ZIF-8 after desorption fits well with that of fresh one, further highlighting on the stability of the adsorbent. Therefore, it is indicated that ZIF-8 adsorbent can be renewed by acetonitrile and shows a great potential for practical application in the gold recovery.

4 Conclusion

The adsorption of Au(III) ions from aqueous solution by ZIF-8 was studied. The adsorption performance containing adsorption capacity and adsorption rate and the recycling use of ZIF-8 toward Au(III) were investigated. The low pH is favorable for the adsorption of Au(III) on ZIF-8 and the Au(III) adsorption process is a spontaneous endothermic process. At 298 K, the maximum adsorption capacity can reach up 1192 mg g^{-1}. The adsorption rate steps are

determined by MD model to be controlled by intraparticle diffusion and chemical interaction. Moreover, ZIF-8 materials could keep stable adsorption properties after recycling use. The preliminary adsorption mechanism was conducted as well. EDS, N_2 adsorption–desorption analysis indicate that Au is doubtlessly attached to the ZIF-8 materials and the main adsorption site is at the internal surface of pores. The adsorption kinetics fits the pseudo-second-order kinetics model well, indicating that the chemisorption exits in the adsorption process, which is confirmed by XPS analysis. Combining the isotherm model, pH-independent adsorption experiment, Au(III) species distribution and point of zero charge of ZIF-8, electrostatic interaction mechanism is revealed, which plays a vital role in the adsorption process. Further research is needed to enhance the adsorption performance, which will make ZIF-8 become a more effective and extensive precious metal adsorption material.

References

Akpomie, G.K., Abuh, M.A., Ogbu, C.I., Agulanna, A.C., Ekpe, I.O.: Adsorption of Cd(II) from solution by Nsu clay: kinetic and thermodynamic studies. J. Emerg. Trend. Eng. Appl. Sci. **3**, 254–258 (2012)

And, L.H.D., Nuzzo, R.G.: Synthesis, structure, and properties of model organic surfaces. Annu. Rev. Phys. Chem. **43**, 437–463 (1992)

Biggar, J.W., Cheung, M.W.: Adsorption of picloram (4-amino-3, 5, 6-trichloropicolinic acid) on panoche, ephrata, and palouse soils: a thermodynamic approach to the adsorption mechanism 1. Soil Sci. Soc. Am. J. **37**, 863–868 (1973)

Chand, R., Watari, T., Inoue, K., Kawakita, H., Luitel, H.N., Parajuli, D., Torikai, T., Yada, M.: Selective adsorption of precious metals from hydrochloric acid solutions using porous carbon prepared from barley straw and rice husk. Miner. Eng. **22**, 1277–1282 (2009)

Chen, X., Lam, K.F., Mak, S.F., Yeung, K.L.: Precious metal recovery by selective adsorption using biosorbents. J. Hazard. Mater. **186**, 902–910 (2011)

Chizallet, C., Lazare, S., Bazer-Bachi, D., Bonnier, F., Lecocq, V., Soyer, E., Quoineaud, A.A., Bats, N.: Catalysis of transesterification by a nonfunctionalized metal—organic framework: acido-basicity at the external surface of ZIF-8 probed by FTIR and ab initio calculations. J. Am. Chem. Soc. **132**, 12365–12377 (2010)

Cui, Y., Yue, Y., Qian, G., Chen, B.: Luminescent functional metal-organic frameworks. Chem. Rev. **112**, 1126–1162 (2012)

Dobson, R.S., Burgess, J.E.: Biological treatment of precious metal refinery waste water: a review. Miner. Eng. **20**, 519–532 (2007)

Dwivedi, A.D., Dubey, S.P, Hokkanen, S., Fallah, R.N., Sillanpää, M.: Recovery of gold from aqueous solutions by taurine modified cellulose: an adsorptive–reduction pathway. Chem. Eng. J. **255**, 97–106 (2014)

Fleming, C.A., Mezei, A., Bourricaudy, E., Canizares, M., Ashbury, M.: Factors influencing the rate of gold cyanide leaching and

adsorption on activated carbon, and their impact on the design of CIL and CIP circuits. Miner. Eng. **24**, 484–494 (2011)

Ghosh, S.K.: Metal–organic frameworks (MOFs) for sensing applications. Acta. Crystallogr. **73**, C1329–C1329 (2017)

Gücüyener, C., van den Bergh, J., Gascon, J., Kapteijn, F.: Ethane/ethene separation turned on its head: selective ethane adsorption on the metal-organic framework ZIF-7 through a gate-opening mechanism. J. Am. Chem. Soc. **132**, 17704–17706 (2010)

Gwak, G., Kim, D.I., Hong, S.: New industrial application of forward osmosis (FO): precious metal recovery from printed circuit board (PCB) plant wastewater. J. Membr. Sci. **552**, 234–242 (2018)

He, M., Yao, J., Liu, Q., Wang, K., Chen, F., Wang, H.: Facile synthesis of zeolitic imidazolate framework-8 from a concentrated aqueous solution. Microporous Mesoporous Mater. **184**, 55–60 (2014)

Ho, Y.S., McKay, G.: Pseudo-second order model for sorption processes. Process Biochem. **34**, 451–465 (1999)

Horcajada, P., Gref, R., Baati, T., Allan, P., Maurin, G., Couvreur, P., Férey, G., Morris, R., Serre, C.: Metal-organic frameworks in biomedicine. Chem. Rev. **112**, 1232–1268 (2012)

Hu, Y., Kazemian, H., Rohani, S., Huang, Y., Song, Y.: In situ high pressure study of ZIF-8 by FTIR spectroscopy. Chem. Commun. **47**, 12694–12696 (2011)

Huo, S.H., Yan, X.P.: Metal-organic framework MIL-100 (Fe) for the adsorption of malachite green from aqueous solution. J. Mater. Chem. **22**, 7449–7455 (2012)

Jian, M., Liu, B., Zhang, G., Liu, R., Zhang, X.: Adsorptive removal of arsenic from aqueous solution by zeolitic imidazolate framework-8 (ZIF-8) nanoparticles. Colloid. Surf. A **465**, 67–76 (2015)

Jiang, J., Yang, C., Yan, X.: Zeolitic imidazolate framework-8 for fast adsorption and removal of benzotriazoles from aqueous solution. ACS Appl. Mater. Inter. **5**, 9837–9842 (2013)

Jiang, L., Zhang, W., Luo, C., Cheng, D., Zhu, J.: Adsorption toward trivalent rare earth element from aqueous solution by zeolitic imidazolate frameworks. Ind. Eng. Chem. Res. **55**, 6365–6372 (2016)

Kavakli, C., Malci, S., Tuncel, S.A., Salish, B.: Selective adsorption and recovery of precious metal ions from geological samples by 1,5,9,13-tetrathiacyclohexadecane-3,11-diol anchored poly(p-CMS-DVB) microbeads. React. Funct. Polym. **66**, 275–285 (2006)

Li, J., Sculley, J., Zhou, H.: Metal-organic frameworks for separations. Chem. Rev. **112**, 869–932 (2011)

Li, J., Wu, Y., Li, Z., Zhang, B., Zhu, M., Hu, X., Zhang, M., Li, F.: Zeolitic imidazolate framework8 with high efficiency in trace arsenate adsorption and removal from water. J. Phys. Chem. C **118**, 27382–27387 (2014)

Lin, S., Reddy, D.H.K., Bediako, J.K., Song, M.H., Wei, W., Kim, J.A., Yun, Y.S.: Effective adsorption of Pd(II), Pt(IV) and Au(III) by Zr(IV)-based metalorganic frameworks from strongly acidic solutions. J. Mater. Chem. A **5**, 13557–13564 (2017)

Liu, H., Cai, X., Wang, Y., Wang, Y., Chen, J.: Adsorption mechanism-based screening of cyclodextrin polymers for adsorption and separation of pesticides from water. Water Res. **45**, 3499–3511 (2011)

Liu, B., Jian, M., Liu, R., Yao, J., Zhang, X.: Highly efficient removal of arsenic(III) from aqueous solution by zeolitic imidazolate frameworks with different morphology. Colloid. Surf. A **481**, 358–366 (2015)

Lyu, J., Liu, H., Zeng, Z., Zhang, J., Xiao, Z., Bai, P., Guo, X.: Metal-organic framework UiO-66 as an efficient adsorbent for boron removal from aqueous solution. Ind. Eng. Chem. Res. **56**, 2565–2572 (2017)

Maruyama, T., Terashima, Y., Takeda, S., Okazaki, F., Goto, M.: Selective adsorption and recovery of precious metal ions using protein-rich biomass as efficient adsorbents. Process Biochem. **49**, 850–857 (2014)

Mironov, I.V., Makotchenko, E.V.: The hydrolysis of $AuCl_4^-$ and the stability of aquachlorohydroxo complexes of gold (III) in aqueous solution. J. Solution Chem. **38**, 725–737 (2009)

Mpinga, C.N., Bradshaw, S.M., Akdogan, G., Snyders, C.A., Eksteen, J.J.: The extraction of Pt, Pd and Au from an alkaline cyanide simulated heap leachate by granular activated carbon. Miner. Eng. **55**, 11–17 (2014)

Ngah, W.S.W., Liang, K.H.: Adsorption of gold(III) ions onto chitosan and NCarboxymethyl chitosan: equilibrium studies. Ind. Eng. Res. **38**, 1411–1414 (1999)

Niknam, S.M., Ghahramaninezhad, M., Eydifarash, M.: Zeolitic imidazolate framework-8 for efficient adsorption and removal of Cr(VI) ions from aqueous solution. Environ. Sci. Pollut. Res. **24**, 9624–9634 (2017)

Ogata, T., Nakano, Y.: Mechanisms of gold recovery from aqueous solutions using a novel tannin gel adsorbent synthesized from natural condensed tannin. Water Res. **39**, 4281–4286 (2005)

Ramesh, A., Hasegawa, H., Sugimoto, W., Maki, T., Ueda, K.: Adsorption of gold (III), platinum (IV) and palladium (II) onto glycine modified crosslinked Chitosan resin. Bioresour. Technol. **99**, 3801–3838 (2008)

Robb, W.: Kinetics and mechanisms of reactions of gold (III) complexes. I. The equilibrium hydrolysis of tetrachlorogold (III) in acid medium. Inorg. Chem. **6**, 382–386 (1967)

Shams, K., Goodarzi, F.: Improved and selective platinum recovery from spent α-alumina supported catalysts using pretreated anionic ion exchange resin. J. Hazard. Mater. **131**, 229–237 (2006)

Shen, K., Zhang, L., Chen, X., Liu, L., Zhang, D., Han, Y., Chen, J., Lomg, J., Luque, R., Li, Y., Chen, B.: Ordered macro-microporous metal-organic framework single crystals. Science **359**, 206–210 (2018)

Sumida, K., Rogow, D.L., Mason, J.A., Mcdonald, T.M., Bloch, E.D., Herm, Z.R., Bae, T.H., Long, J.R.: Carbon dioxide capture in metal-organic frameworks. Chem. Rev. **112**, 724–781 (2011)

Wang, M., Tan, Q., Chiang, J.F., Li, J.: Recovery of rare and precious metals from urban mines—a review. Front. Env. Sci. Eng. **11**, 1–17 (2017)

Wang, Z., Zhang, B., Ye, C., Chen, L.: Recovery of Au(III) from leach solutions using thiourea functionalized zeolitic imidazolate frameworks (TU*ZIF-8). Hydrometallur **180**, 262–270 (2018)

Won, S.W., Kotte, P., Wei, W., Lim, A., Yun, Y.S.: Biosorbents for recovery of precious metals. Bioresour. Technol. **160**, 203–212 (2014)

Wu, C., Zhu, X., Wang, Z., Yang, J., Li, Y., Gu, J.: Specific recovery and in situ reduction of precious metal from waste to create MOF composites with immobilized nanoclusters. Ind. Eng. Chem. Res. **56**, 13975–13982 (2017)

Zha, M., Liu, J., Wong, Y.L., Xu, Z.: Extraction of palladium from nuclear waste-like acidic solutions by a metal-organic framework with sulfur and alkene functions. J. Mater. Chem. A **3**, 3928–3934 (2015)

Zhang, L., Xu, Z.: A review of current progress of recycling technologies for metals from waste electrical and electronic equipment. J. Clean. Prod. **127**, 19–36 (2016)

Zhang, Z., Xian, S., Xia, Q., Wang, H., Li, Z., Li, J.: Enhancement of CO_2 adsorption and CO_2/N_2 selectivity on ZIF-8 via postsynthetic modification. AIChE J. **59**, 2195–2206 (2013)

Zhang, F., Zheng, Y., Sun, Z., Ma, Y., Dong, J.: Recovery of rare and precious metals from precipitated gold solution by Na_2SO_3 reduction. Chin. J. Nonferrous Met. **25**, 2293–2299 (2015)